Title

MATHEMATICAL MODELING OF LIQUID-JUNCTION PHOTOVOLTAIC CELLS: I. GOVERNING EQUATIONS

Authors

Orazem, M.E.
Newman, J.

Publication Date

1983-06-01

Lawrence Berkeley Laboratory
UNIVERSITY OF CALIFORNIA

Materials & Molecular Research Division

Submitted to the Journal of the Electrochemical Society

MATHEMATICAL MODELING OF LIQUID-JUNCTION PHOTOVOLTAIC CELLS: I. GOVERNING EQUATIONS

M.E. Orazem and J. Newman

June 1983

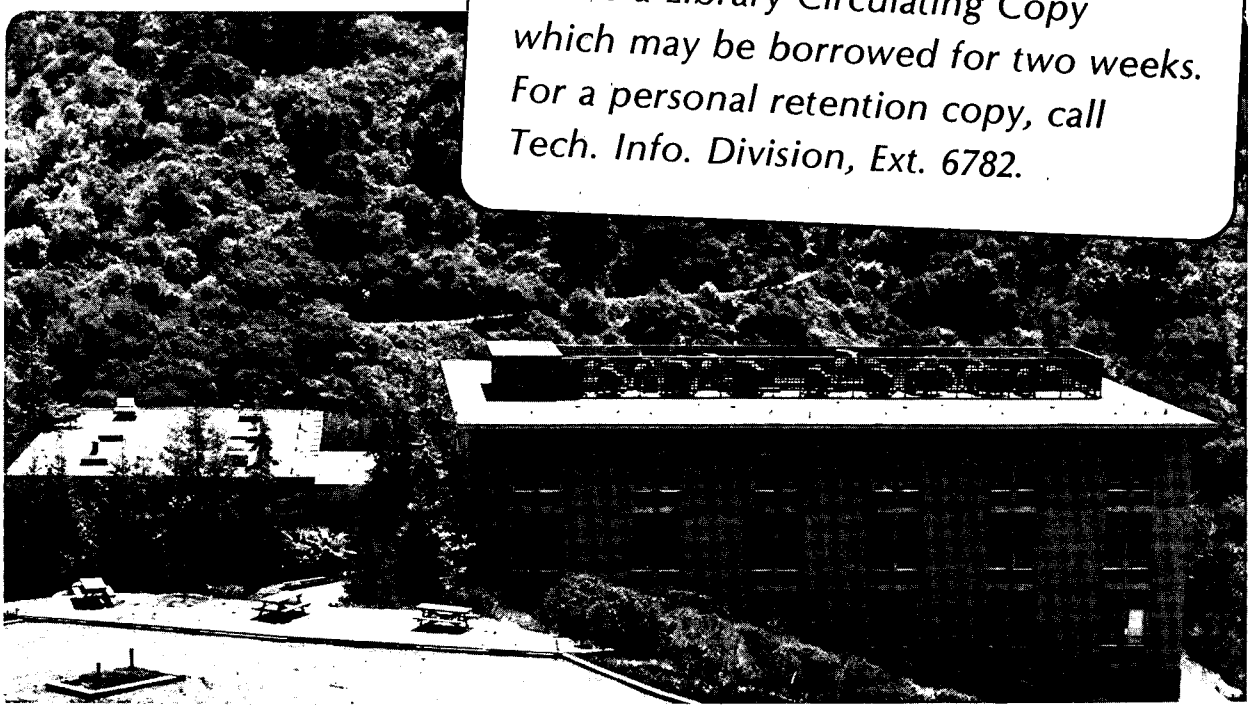

Prepared for the U.S. Department of Energy under Contract DE-AC03-76SF00098

DISCLAIMER

LBL-16210

Mathematical Modeling of Liquid-Junction Photovoltaic Cells:

I. Governing Equations

Mark E. Orazem and John Newman

Materials and Molecular Research Division, Lawrence Berkeley Laboratory, and Department of Chemical Engineering, University of California, Berkeley, California 94720

June 1983

ABSTRACT

The equations which govern the liquid-junction photovoltaic cell are presented in the context of a one-dimensional mathematical model. This model treats explicitly the semiconductor, the electrolyte, and the semiconductor-electrolyte interface in terms of potentials and concentrations of charged species. The model incorporates macroscopic transport equations in the bulk of the semiconductor and electrolyte coupled with a microscopic model of the semiconductor-electrolyte interface. Homogeneous and heterogeneous recombination of electron-hole pairs is included within the model. Recombination takes place at the semiconductor-electrolyte interface through interfacial sites, which can enhance the recombination rate. The coupled nonlinear ordinary differential equations of the model were posed in finite-difference form and solved numerically. The results are presented in succeeding papers.[44,45]

Key words: Semiconductor, Electrode, Solar, Energy Conversion.

The liquid-junction photovoltaic cell is an electrochemical system with one or two semiconducting electrodes. This system has undergone intense study since the early 1970's as a means of converting solar energy to chemical or electrical energy.[1-8] A number of articles review the physics of the liquid-junction cell, the role of the semiconducting electrode, and the literature (see, e.g., references 9-19).

A mathematical model is presented here which treats explicitly all components of the liquid-junction photovoltaic cell. The results of the model, obtained through numerical computation, are used to gain insight into the cell behavior and into the factors influencing cell design.

1. INTRODUCTION

Development of a mathematical model constitutes an important step toward understanding the behavior and predicting the performance of the liquid-junction photovoltaic cell. Coupled phenomena govern the system, and the equations describing their interaction cannot, in general, be solved analytically. Two approaches have been taken in developing a mathematical model of the liquid-junction photovoltaic cell: approximate analytic solution of the governing equations and numerical solution. These are reviewed elsewhere.[20]

Use of a digital computer in the numerical solution of the equations governing the liquid-junction cell eliminates the need for restrictive assumptions. The numerical approach was taken in this work[20] and has been used in the modeling of solid-state devices.[21-26] Laser and Bard[27-30] developed a computer program which was used to calculate open-circuit photopotentials, the transient behavior of the system following charge injection, and the time dependence of photocurrents in liquid-junction cells.

Time dependent material balances of holes and electrons and Poisson's equation described the semiconductor. The interface was included in terms of charge and flux boundary conditions. The model was limited by lack of convergence for electrode thicknesses greater than that of the space-charge region and did not treat explicitly the electrolyte and counterelectrode.

A number of computer programs related to the liquid-junction photovoltaic cell have been developed. Leary *et al.*,[31] for example, calculated carrier concentrations in polycrystalline films using a numerical solution of Poisson's equation coupled with overall charge neutrality within spherical grains. Their model was used for analysis of semiconductor gas sensors. A computer program has been presented by Davis and colleagues[32-34] which uses simultaneous calculation of surface and solution equilibrium states to obtain the equilibrium condition of electrical double layers.

2. PHYSICAL MODEL

A one-dimensional representation of the liquid-junction photovoltaic cell is presented in Figure 1. This model includes macroscopic representations of the counterelectrode, the electrolytic solution, and the semiconductor coupled with a microscopic representation of the interface between the semiconductor and the solution. The semiconductor-electrolyte interface couples the macroscopic equations which govern the adjacent bulk phases.

The interface is represented by four planes, inner and outer Helmholtz planes on the electrolyte side of the interface and inner and outer surface states on the semiconductor side. The outer Helmholtz plane (OHP) is the

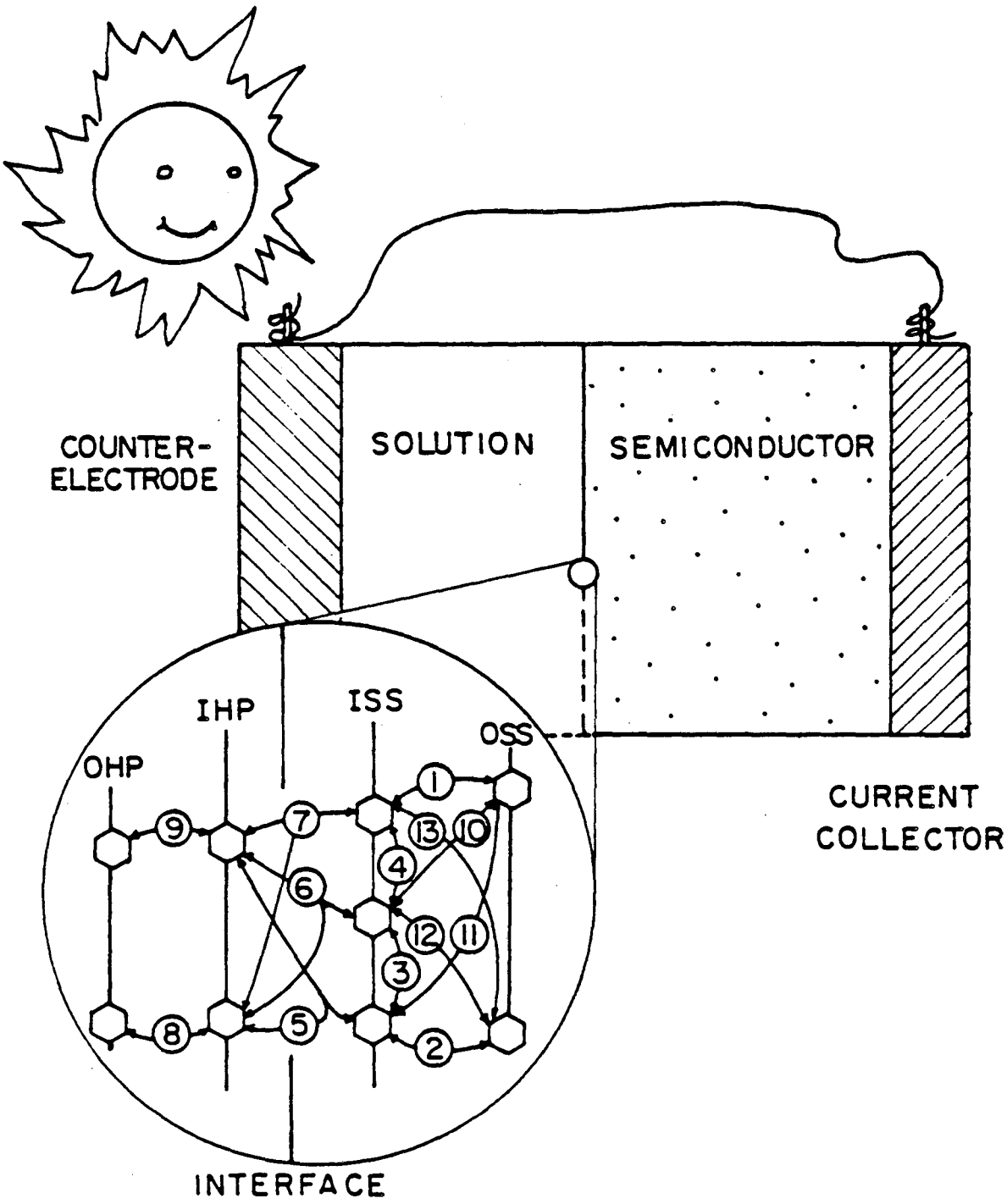

XBL 835-9621

Figure 1. Mathematical model of the liquid-junction photovoltaic cell.

plane of closest approach for (hydrated) ions associated with the bulk solution. The inner Helmholtz plane (IHP) passes through the center of ions specifically adsorbed on the semiconductor surface. The outer surface state (OSS) represents the plane of closest approach for electrons (and holes) associated with the bulk of the semiconductor. The inner surface state (ISS) is a plane of surface sites for adsorbed electrons.

This model of the semiconductor-electrolyte interface is an extension of the classical diffuse double-layer theory.[35-37] Charge adsorbed onto the IHP and the ISS planes is balanced by charge in the diffuse region of the electrolyte and the space-charge region of the semiconductor. The net charge of the interface, including surface planes and diffuse and space-charge regions, is equal to zero.

Within the model, single-step reactions relate concentrations and potentials at interfacial planes. A continuous spectrum of energy levels at the ISS is represented by three discrete energy levels (designated v, t, and c). Conduction electrons are adsorbed via reaction 1 (see INTERFACE in Figure 1) from the OSS to high-energy sites at the ISS, via reaction 10 to intermediate-energy sites at the ISS, and via reaction 11 to low-energy sites at the ISS. Via reaction 2, low-energy electrons at the ISS can occupy vacancies in the valence band, or holes, at the OSS. Intermediate-energy electrons can transfer from the ISS to the OSS through reaction 12 and high-energy electrons can transfer through reaction 13. Reactions 3 and 4 allow the shifting of electrons from one energy level to another.

Ionic species from the solution are adsorbed onto the IHP by reactions 8 and 9. Two adsorbed species are considered here. It is assumed that other ionic species in the solution do not adsorb and do not participate in

the electrochemical reactions. Relaxation of this assumption involves the inclusion of additional ion-adsorption and charge-transfer reactions. Reactions 5, 6, and 7 are the charge-transfer reactions that take place among adsorbed ions at the IHP and adsorbed high, intermediate, or low-energy electrons at the ISS. Charge-transfer reactions allow passage of electrical current from the semiconductor to the solution.

3. THEORETICAL DEVELOPMENT

The equations governing the liquid-junction photovoltaic cell in the dark or under steady-state illumination are developed here in terms of the model presented above. The governing relationships can be developed separately for the semiconductor and the electrolyte. The microscopic model of the semiconductor-electrolyte interface couples the equations governing the macroscopic systems.

3.1. Semiconductor

The electrochemical potential of a given species can arbitrarily be separated into terms representing a reference state, a chemical contribution, and an electrical contribution.

$$\mu_i = \mu_i^{\vartheta} + RT\, ln(c_i f_i) + z_i F \Phi\,, \qquad (2)$$

where Φ is a potential which characterizes the electrical state of the phase and can be arbitrarily defined. The potential used here is the electrostatic potential which is obtained through integration of Poisson's equation.[38] Equation (2) can be viewed as the defining equation for the activity coefficient, f_i.

The flux of an individual species within the semiconductor is driven by a gradient of electrochemical potential, which corresponds to gradients of

potential and concentration (see, e.g., Chapter 11 in reference (39) and Gerischer[40]). Under the assumption that the individual ionic activity coefficients are constant with a value of one,* the flux of holes is given by

$$N_{h^+} = -u_{h^+} F p \frac{d\Phi}{dy} - D_{h^+} \frac{dp}{dy} , \tag{3}$$

and the flux of electrons by

$$N_{e^-} = u_{e^-} F n \frac{d\Phi}{dy} - D_{e^-} \frac{dn}{dy} . \tag{4}$$

The concentrations of electrons and holes are represented by n and p, respectively, and the mobilities u_i are related to the diffusivities D_i by the Nernst-Einstein equation

$$D_i = RTu_i . \tag{5}$$

Homogeneous reaction takes place in the semiconductor; thus a material balance for a given species, say holes,** yields

$$\frac{dN_{h^+}}{dy} = R_{h^+} , \tag{6}$$

where R_{h^+} is the net rate of production of holes under steady-state conditions.

The rate of production of holes is, by stoichiometry, equal to the rate of production of electrons and is governed by three concurrent processes: generation by absorption of light, generation by absorption of heat, and recombination of electrons and holes (i.e., transfer of an electron from the conduction band to the valence band).

---

* The assumption of constant activity coefficients, valid for dilute solutions, is appropriate for most semiconductors. The carrier concentrations in semiconductors is usually less than 0.0001 M, which is low as compared to dilute aqueous solutions. The assumption of constant activity coefficients is in harmony with a Boltzmann distribution of electrons and holes. Use of Fermi-Dirac distributions for these charged species results in activity coefficients that are functions of concentration (see Chapter 6 in reference (20)).

** The development presented here, while applicable to p-type semiconductors, is oriented toward analysis of an n-type semiconductor in which holes are the minority carrier. Material balances of holes and electrons are not independent, and conservation of the minority carrier was chosen to improve the numerical computational accuracy.

$$R_{h^+} = G_L + G_{th} - R_{rec} \quad . \tag{7}$$

Mathematical models of the homogeneous recombination process have been developed which incorporate single-step electron transfer from one energy level to another. They differ in the assumption of the presence or absence of impurities within the semiconductor which allow electrons to have energies between the conduction and valence-band energies.[41,42]

Band-to-band kinetic models (presented in Figure 2) allow electrons to have only valence or conduction-band energies. Absorption of the appropriate amount of thermal or electromagnetic energy creates an electron-hole pair; recombination of an electron and a hole releases energy in the form of heat or light. The band-to-band model yields

$$R_{h^+} = \eta m q_o e^{-my} - k_{rec}(np - n_i^2) \quad , \tag{8}$$

where η is the fraction of incident photons with energy greater than the band gap energy, m is the absorption coefficient, q_o is the incident solar flux, and n_i is the intrinsic concentration,

$$n_i = \left[\frac{k_{th}(N_c - n)(N_v - p)}{k_{rec}}\right]^{1/2} \tag{9}$$

The intrinsic concentration is written in terms of N_c and N_v, the number of available conduction and valence-band sites respectively, and k_{th} and k_{rec}, thermal generation and recombination rate constants. Under equilibrium conditions, the rate of thermal generation is equal to the rate of recombination, and $np = n_i^2$.

Most semiconducting materials contain impurities or imperfections within their lattice structure which may be described as fixed sites with valence-band electron energies within the semiconductor band gap. The trap-kinetics model allows recombination to occur through these sites (see Figure 3). Absorbed radiation drives an electron from the valence band to

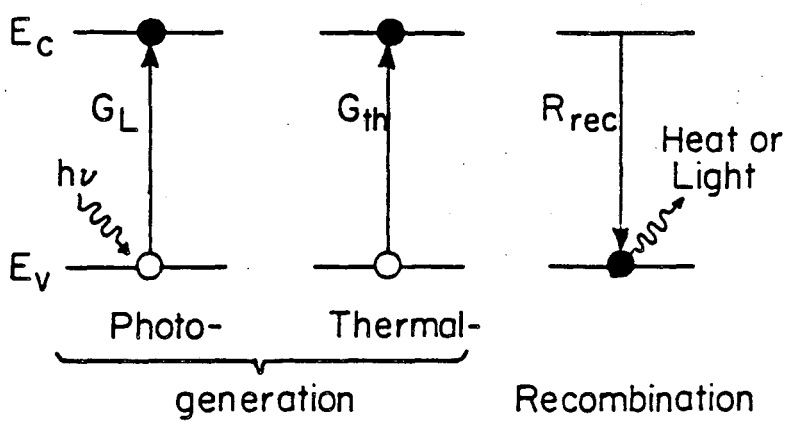

Individual Reaction Rates

$$G_L = \eta m q_o e^{-mx}$$

$$G_{th} = k_{th}(N_c - n)(N_v - p)$$

$$R_{rec} = k_{rec}\, np$$

XBL 831-5023

Figure 2. Schematic representation of band-to-band recombination kinetics in the semiconductor.

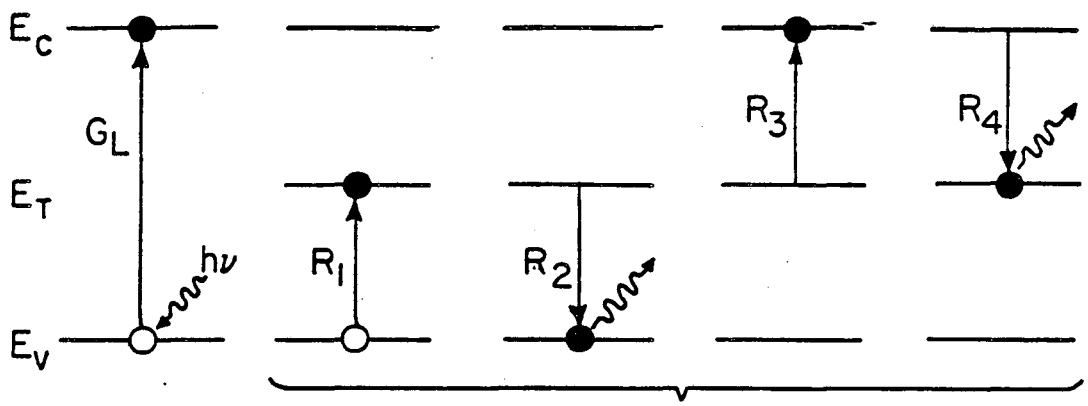

Thermal Generation and Recombination
Through Trap Sites

Individual Reaction Rates

$$G_L = \eta m q_o e^{-mx}$$

$$R_1 = k_1(N_V - p)(N_T - n_T)$$

$$R_2 = k_2 n_T p$$

$$R_3 = k_3 n_T (N_C - n)$$

$$R_4 = k_4 n (N_T - n_T)$$

XBL 831-5024

Figure 3. Schematic representation of single-trap recombination kinetics in the semiconductor.

the conduction band, and all recombination and thermal generation reactions are assumed to occur through trap sites. This model results in

$$R_{h^+} = \eta m q_o e^{-my} - \frac{N_t k_2 (np - n_i^2)}{\frac{k_1(N_v - p) + k_3(N_c - n)}{k_4} + \frac{k_2}{k_4} p + n}, \qquad (10)$$

where k_1, k_2, k_3, and k_4 are the rate constants for the corresponding reactions shown in Figure 3. The intrinsic concentration is given by

$$n_i = \left[\frac{k_1 k_3 (N_c - n)(N_v - p)}{k_2 k_4} \right]^{1/2}. \qquad (11)$$

The electron and hole concentrations are generally small as compared to the respective conduction and valence-band site concentrations. The intrinsic concentration is therefore constant, and the reaction rate can be characterized with three lumped rate constants ($N_t k_2$, $(k_1 N_v + k_3 N_c)/k_4$, and k_2/k_4). Homogeneous electron-hole recombination was assumed in the mathematical model to occur through trap sites (equations (10) and (11)).

The expressions for the intrinsic concentration (equations (9) and (11)) are consistent with the expression derived through statistical-mechanical models (see equation (32) of Chapter 6, reference (20)). The intrinsic concentration can be considered to be a constant for a given semiconductor only if the ratios n/N_c and p/N_v are negligibly small as compared to unity. This condition is consistent with the assumption of unity activity coefficients for electrons and holes. The value of the intrinsic concentration derived from statistical-mechanical arguments serves as a relationship among the kinetic parameters in equations (9) and (11).

The divergence of the current is zero at steady state; therefore the fluxes of holes and electrons are related by

$$\frac{dN_{e^-}}{dy} - \frac{dN_{h^+}}{dy} = 0 . \qquad (12)$$

A material balance on electrons, analogous to equation (5), could be used to replace equation (12).

Poisson's equation,

$$\frac{d^2\Phi}{dy^2} = - \frac{F}{\varepsilon_{sc}}[\, p - n + (N_d - N_a)\,] , \qquad (13)$$

relates the potential to the charge distribution. The concentrations of ionized electron donors and acceptors are represented by N_d and N_a, respectively. The Debye length,

$$\lambda_{sc} = [\varepsilon_{sc} RT / F^2 (N_d - N_a)]^{1/2} ,$$

characterizes the distance over which the potential varies in the semiconductor. It typically has a value of 1×10^{-6} to 2×10^{-5} cm.

The degree of ionization of donors or acceptors is dependent upon the concentrations of charged species within the semiconductor and upon the temperature. Complete ionization has been assumed in this work. This assumption is reasonable at room temperatures and is consistent with the assumption of unity activity coefficients.

3.2. Electrolyte

For a one-dimensional case, neglecting convective effects, the flux of an ionic species is governed by potential and concentration gradients.

$$N_i = - z_i u_i c_i F \frac{d\Phi}{dy} - D_i \frac{dc_i}{dy} . \qquad (14)$$

Under the assumption that homogeneous reactions do not take place, conservation of mass yields a uniform flux at steady-state, i.e.,

$$\frac{dN_i}{dy} = 0 . \qquad (15)$$

The potential and concentrations of charged species are related by

Poisson's equation,

$$\frac{d^2\Phi}{dy^2} = -\frac{F}{\varepsilon_{sol}} \sum_i z_i c_i \ . \tag{16}$$

Electroneutrality of the electrolyte is not assumed here because the diffuse region near the interface plays an important role in the microscopic model of the interface. The Debye length in the solution is given by

$$\lambda_{sol} = [\varepsilon_{sol} RT / F^2 \sum_i z_i^2 c_{i,\infty}]^{1/2}$$

and typically has a value of 1×10^{-8} to 1×10^{-7} cm.

The relationships presented above are sufficient to describe the electrolytic solution. An additional relationship yields the current density as a function of the ionic fluxes,

$$i = F \sum_i z_i N_i \ . \tag{17}$$

Within the semiconductor, this can be regarded as an integrated form of equation (12).

3.3. Semiconductor-electrolyte interface

A general interfacial reaction can be expressed as

$$\sum_i s_i M_i^{z_i} \rightarrow n e^- \ , \tag{18}$$

where s_i is the stoichiometric coefficient of species i, M_i is a symbol for the chemical formula of species i, and n is the number of electrons transferred. (See Chapter 8 in reference (39).) For single-step reactions, n is equal to one.

The rate of a single-step reaction l at the interface is given by

$$r_l = k_{f,l}\exp\left[\frac{(1-\beta_l)F\Delta\Phi_l}{RT}\right]\prod_i c_i^{p_{i,l}} - k_{b,l}\exp\left[\frac{-\beta_l F\Delta\Phi_l}{RT}\right]\prod_i c_i^{q_{i,l}}, \tag{19}$$

where β_l is a symmetry factor (usually assumed to be equal to 1/2), $k_{f,l}$ and $k_{b,l}$ are forward and backward reaction rate constants, respectively, and $\Delta\Phi_l$ is the potential driving force for the given reaction, l. The potential driving force enters into reactions involving charge transfer from locations of one potential to locations of another.

The reaction orders for a given species i in the forward and reverse directions are $p_{i,l}$ and $q_{i,l}$ respectively. They are determined from the stoichiometric coefficients, $s_{i,l}$:

$$\begin{aligned} &\text{If } s_{i,l} = 0; \quad p_{i,l} = 0, \quad \text{and } q_{i,l} = 0. \\ &\text{If } s_{i,l} > 0; \quad p_{i,l} = s_{i,l}, \text{ and } q_{i,l} = 0. \\ &\text{If } s_{i,l} < 0; \quad p_{i,l} = 0, \quad \text{and } q_{i,l} = -s_{i,l}. \end{aligned}$$

The reaction rates are written in terms of the equilibrium constants as

$$r_l = k_{b,l}\left\{K_l\exp\left[\frac{(1-\beta_l)F\Delta\Phi_l}{RT}\right]\prod_i c_i^{p_{i,l}} - \exp\left[\frac{-\beta_l F\Delta\Phi_l}{RT}\right]\prod_i c_i^{q_{i,l}}\right\}. \tag{20}$$

The equilibrium constant used here is the ratio of the forward and backward rate constants:

$$K_l = \frac{k_{f,l}}{k_{b,l}}. \tag{21}$$

Six of the thirteen equilibrium constants are independent and can be calculated as functions of equilibrium interfacial concentrations and potentials.

$$K_l = \exp[-\frac{F}{RT}\Delta\Phi_l]\prod_i c_i^{-s_{i,l}} \quad (22)$$

A discussion of the calculation of equilibrium concentrations and potentials and the subsequent calculation of equilibrium constants is presented elsewhere (see Chapter 6, reference (20)). The remaining constants can be calculated from equation (22) or from the following identities:

$$K_4 = \frac{K_3(N_d - N_a)^2}{K_1 K_2 n_i^2}, \quad (23a)$$

$$K_6 = K_5 / K_3, \quad (23b)$$

$$K_7 = K_6 / K_4, \quad (23c)$$

$$K_{10} = K_1 K_4, \quad (23d)$$

$$K_{11} = K_{10} / K_3, \quad (23e)$$

$$K_{12} = K_2 / K_3, \quad (23f)$$

and

$$K_{13} = K_{12} K_4. \quad (23g)$$

Within the parametric studies which follow, one independent rate constant is assumed to be characteristic of each of four groups of interfacial reactions. The four groups, shown in Figure 1, are reactions 1, 2, 10, 11, 12, and 13 (OSS-ISS), reactions 3 and 4 (ISS), reactions 5, 6, and 7 (ISS-IHP), and reactions 8 and 9 (IHP-OHP). The individual rate constants for each reaction l are related to the characteristic rate constant by

$$k_{b,l} = k_l^o K_l^{-\beta} \quad (24)$$

and

$$k_{f,l} = k_{b,l} K_l = k_l^o K_l^{1-\beta}, \quad (25)$$

where k_l^o is the pre-exponential part of the rate constant, with a characteristic value for a given reaction type, and β was given a value of one half. These equations are consistent with equations (20) and (21).

Material balances govern the interface under steady-state conditions. These are expressed by continuity of flux at the OSS and the OHP,

$$N_{e^-}\Big|_{oss} = \sum_l -s_{e^-,l}\,r_{l,iss} \ , \tag{26}$$

$$N_{h^+}\Big|_{oss} = \sum_l -s_{h^+,l}\,r_{l,iss} \ , \tag{27}$$

and

$$N_i\Big|_{ohp} = \sum_l -s_{i,l}\,r_l \ ; \tag{28}$$

and material balances for each adsorbed species i at the ISS and the IHP,

$$\sum_l s_{i,l}\,r_{l,iss} = 0 \ , \tag{29}$$

and

$$\sum_l s_{i,l}\,r_{l,ihp} = 0 \ . \tag{30}$$

Gauss's law can be applied to the region between the OSS and ISS:

$$(\Phi_{oss} - \Phi_{iss}) = \frac{\delta_1}{\varepsilon_{sc}}\left[\frac{\varepsilon_2}{\delta_2}(\Phi_{iss} - \Phi_{ihp}) + F(\sum_{iss}\gamma_i - q^+_{iss})\right], \tag{31}$$

and between the ISS and the IHP:

$$(\Phi_{iss} - \Phi_{ihp}) = \frac{\delta_2}{\varepsilon_2}\left[\frac{\varepsilon_{sol}}{\delta_3}(\Phi_{ihp} - \Phi_{ohp}) - F(\sum_{ihp} z_i\gamma_i)\right]. \tag{32}$$

The evaluation of Gauss's law in the region between the OSS and the ISS includes a term for a fixed positive charge at the ISS, q^+_{iss}, which was set equal to zero in this study.

3.4. Boundary conditions

The semiconducting electrode is bounded at one end by the electrolyte and at the other end by a metallic current collector. The boundary conditions at the semiconductor-electrolyte interface are incorporated into the model of the interface. The boundary conditions at the semiconductor-current collector interface are that the potential is zero, the potential

derivative is equal to a constant, determined by the charge assumed to be located at the semiconductor-current collector interface (this constant was set equal to zero in this study), and all the current is carried by electrons (the flux of holes is zero). The boundary conditions in the electrolytic solution are set a fixed distance (10 Debye lengths) from the interface. This distance may be considered to be a diffusion layer. The boundary conditions are that the potential gradient is continuous and that all concentrations have their bulk value.

3.5. Counterelectrode

In the region sufficiently far from the interface that electroneutrality holds, the potential distribution is linear and is a function of current density. The potential drop in the region between the counterelectrode and the outer limit of the diffusion layer is given by

$$V_{IR} = \frac{Li}{\kappa}, \tag{33}$$

where κ is the solution conductivity and L is the distance between the counterelectrode and the outer edge of the diffusion layer. The conductivity of dilute solutions is related to ionic mobilities and concentrations by

$$\kappa = F^2 \sum_i z_i^2 u_i c_i . \tag{34}$$

The potential drop across the counterelectrode-electrolyte interface is given by

$$V_{CE} = V_{CE}^o + \eta_{CE} , \tag{35}$$

where V_{CE}^o is the equilibrium potential drop across the interface and η_{CE} is the total counterelectrode reaction overpotential. The total overpotential is related to the current density through the Butler-Volmer reaction

model;[39,43]

$$i = i_o \left\{ \left[1 - \frac{i}{i_{4,lim}} \right] \exp\left[\frac{(1-\beta)nF}{RT} \eta_{CE} \right] - \left[1 + \frac{i}{i_{3,lim}} \right] \exp\left[- \frac{\beta n F}{RT} \eta_{CE} \right] \right\}, \tag{36}$$

where i_o is the exchange current density associated with the bulk concentrations of reactants, $i_{k,lim}$ is the diffusion-limited current density associated with species k, and n is the number of electrons transferred in the counterelectrode reaction.

4. CONCLUSION

The equations which govern the liquid-junction photovoltaic cell are presented in the context of a one-dimensional mathematical model. This model treats explicitly the semiconductor, the electrolyte, and the semiconductor-electrolyte interface in terms of potentials and concentrations of charged species. The model incorporates macroscopic transport equations in the bulk of the semiconductor and electrolyte coupled with a microscopic model of the semiconductor-electrolyte interface. Homogeneous and heterogeneous recombination of electron-hole pairs is included within the model. Recombination takes place at the semiconductor-electrolyte interface through interfacial sites, which can enhance the recombination rate. The coupled nonlinear ordinary differential equations of the model were posed in finite-difference form and solved numerically. Such numerical solution of the governing equations reduces the number of restrictive assumptions needed to solve the problem. The model can be used to gain insight into the effect of cell parameters on

cell performance[44] and can be coupled with primary resistance calculations to optimize cell configurations.[45]

5. ACKNOWLEDGEMENT

This work was supported by the United States Department of Energy under Contract No. DE-AC03-76SF00098 through the Director, Office of Energy Research, Office of Basic Energy Sciences, Chemical Sciences Division, and through the Assistant Secretary of Conservation and Renewable Energy, Office of Advanced Conservation Technology, Electrochemical Systems Research Division.

6. NOTATION

6.1. Roman Characters

c_i	molar concentration of species i, mol/cm^3
D_i	diffusivity of species i, cm^2/s
E_i	energy of species or site i, eV
ΔE_i	ionic adsorption energy, J/mol
f_i	molar activity coefficient of species i
F	Faraday's constant, 96,487 C/equiv
G_{th}	rate of thermal electron-hole pair generation, mol/s-cm^3
G_L	rate of photo electron-hole pair generation, mol/s-cm^3
i	current density, mA/cm^2
i_o	exchange current density, mA/cm^2
$k_{f,l}$	forward reaction rate constant for reaction l
$k_{b,l}$	backward reaction rate constant for reaction l
k_k	rate constants for homogeneous reaction k
K_l	equilibrium constant for reaction l
m	solar absorption coefficient, 1/cm
M_i	symbol for chemical formula of species i
n	number of electrons involved in electrode reaction
n	electron concentration, mol/cm^3
n_i	intrinsic electron concentration, mol/cm^3
N	total site concentration, mol/cm^3
N_a	total bulk electron-acceptor concentration, mol/cm^3
N_d	total bulk electron-donor concentration, mol/cm^3
N_i	flux of species i, mol/cm^{2}s

p	hole concentration, mol/cm^3
$p_{i,l}$	heterogeneous reaction order
$q_{i,l}$	heterogeneous reaction order
q_o	incident solar flux, mol/s-cm^2
r_l	heterogeneous reaction rate, mol/s-cm^2
R	universal gas constant, 8.3143 J/mol-K
R_i	net rate of production of species i, mol/s-cm^3
R_{rec}	net rate of electron-hole recombination, mol/s-cm^3
s_i	stoichiometric coefficient of species i in an electrode reaction
T	absolute temperature, K
u_i	mobility of species i, cm^2-mol/J-s
V	potential drop across depletion layer, V
W	depletion layer thickness, cm
y	distance variable, cm
z_i	charge number of species i

6.2. Greek Characters

β	symmetry factor
γ_k	surface concentration of energy or species k, mol/cm^2
Γ_k	total surface-site concentration of energy or species k, mol/cm^2
δ_k	distance between interfacial planes (gap denoted by k), cm
ε	permittivity, C/V-cm
η	photon efficiency
η_k	total overpotential at interface k, V
Θ	fractional occupation of surface sites
κ	conductivity, mho/cm

λ	Debye length, cm
μ_i	electrochemical potential of species i, J/mol
Φ	electrical potential, V

6.3. Superscripts

o	equilibrium
ϑ	secondary reference state at infinite dilution
$*$	secondary reference state in semiconductor

6.4. Subscripts

bulk	associated with the bulk
c	associated with conduction band in semiconductor
CE	associated with the counterelectrode
cell	associated with the cell
e^-	relating to electrons
h^+	relating to holes
ihp	associated with inner Helmholtz plane
iss	associated with inner surface states
k	dummy subscript
l	associated with reaction *l*
o	equilibrium value or initial value
ohp	associated with outer Helmholtz plane
oss	associated with outer surface states
sc	associated with semiconductor
sol	associated with solution
t	associated with trap band in semiconductor

v	associated with valence band in semiconductor
1	associated with the region between the OSS and the ISS
2	associated with the region between the ISS and the IHP
3	associated with the region between the IHP and the OHP

7. REFERENCES

[1] Fujishima, Akira, and Kenichi Honda, "Electrochemical Photolysis of Water at a Semiconductor Electrode," *Nature*, *238* (1972), 37-38.

[2] Manassen, J., D. Cahen, and G. Hodes, "Electrochemical, Solid State, Photochemical, and Technological Aspects of Photoelectrochemical Energy Converters," *Nature*, *263* (1976), 97-100.

[3] Bard, Allen J., "Photoelectrochemistry and Heterogeneous Photocatalysis at Semiconductors," *Journal of Photochemistry*, *10* (1979), 59-75.

[4] Ehrenreich, H. and J. H. Martin, "Solar Photovoltaic Energy," *Physics Today*, *32*, 9 (1979), 25-32.

[5] Wrighton, Mark S., "Photoelectrochemical Conversion of Optical Energy to Electricity and Fuels," *Accounts of Chemical Research*, *12* (1979), 303-310.

[6] Gerischer, Heinz, "Heterogeneous Electrochemical Systems for Solar Energy Conversion," *Pure and Applied Chemistry*, *52* (1980), 2649-2667.

[7] Bard, Allen J., "Photoelectrochemistry," *Science*, *207* (1980), 139-144.

[8] Heller, Adam, "Conversion of Sunlight into Electrical Power and Photoassisted Electrolysis of Water in Photoelectrochemical Cells," *Accounts of Chemical Research*, *14* (1981), 154-162.

[9] Green, Mino, "Electrochemistry of the Semiconductor-Electrolyte Interface," Chapter 5 in *Modern Aspects of Electrochemistry*, Volume 2, J. O'M Bockris, editor, Academic Press Inc., New York, 1959.

[10] Gerischer, Heinz, "Semiconductor Electrode Reactions," Chapter 4 in *Advances in Electrochemistry and Electrochemical Engineering*, Volume 1, Paul Delahay, editor, Interscience Publishers, New York, 1961.

[11] Archer, M.D., "Electrochemical Aspects of Solar Energy Conversion," *Journal of Applied Electrochemistry*, *5* (1975), 17-38.

[12] Rajeshwar, K., P. Singh, and J. DuBow, "Energy Conversion in Photoelectrochemical Systems: A review," *Electrochimica Acta*, *23* (1975), 1117-1144.

[13] Harris, L. A., and R. H. Wilson, "Semiconductors for Photoelectrolysis," *Annual Reviews in Materials Science*, *8* (1978), 99-134.

[14] Nozik, Arthur, J., "Photoelectrochemistry: Applications to Solar Energy Conversion," *Annual Reviews in Physical Chemistry*, *29* (1978), 189-222.

[15] Tomkiewicz, M., and H. Fay, "Photoelectrolysis of Water with Semiconductors," *Applied Physics*, *18* (1979), 1-28.

[16] Wilson, R.H., "Electron Transfer Processes at the Semiconductor-Electrolyte Interface," *CRC Critical Reviews in Solid State and Materials*

Science, (1980), 1-41.

[17] Memming, R., "Solar Energy Conversion by Photoelectrochemical Processes," *Electrochimica Acta*, *25* (1980), 77-88.

[18] Morrison, S. Roy, *Electrochemistry at Semiconductor and Oxidized Metal Electrodes*, Plenum Press, New York, 1980.

[19] Khan, Shahed U. M., and John O'M. Bockris, "Photoelectrochemical Kinetics and Related Devices," Chapter 3 in *Modern Aspects of Electrochemistry*, Volume 14, J. O'M. Bockris, B. E. Conway, and R. E. White, editors, Plenum Press, New York, 1982.

[20] Orazem, Mark Edward, *Mathematical Modeling and Optimization of Liquid-Junction Photovoltaic Cells*, PhD thesis, University of California, Berkeley, June, 1983 (LBL-16131).

[21] Macdonald, J. Ross, "Accurate Solution of an Idealized One-Carrier Metal-Semiconductor Junction Problem," *Solid-State Electronics*, *5* (1962), 11-37.

[22] De Mari, A., "An Accurate Numerical Steady-State One-Dimensional Solution of the p-n Junction," *Solid-State Electronics*, *11* (1968), 33-58.

[23] De Mari, A., "An Accurate Numerical Steady-State One-Dimensional Solution of the p-n Junction under Arbitrary Transient Conditions," *Solid-State Electronics*, *11* (1968), 1021-1053.

[24] Choo, Seok Cheow, "Numerical Analysis of a Forward-Biased Step-Junction p-i-n Diode," *IEEE Transactions on Electron Devices*, *ED-18* (1971), 574-586.

[25] Choo, Seok Cheow, "Theory of a Forward-Biased Diffused-Junction p-i-n Rectifier-Part 1: Exact Numerical Solution," *IEEE Transactions on Electron Devices*, *ED-19* (1972), 954-966.

[26] Sutherland, J. E., and J. R. Hauser, "A Computer Analysis of Heterojunction and Graded Composition Solar Cells," *IEEE Transactions on Electron Devices*, *ED-24* (1977), 363-372.

[27] Laser, Daniel, and Allen J. Bard, "Semiconductor Electrodes: VII. Digital Simulation of Charge Injection and the Establishment of the Space Charge Region in the Absence and Presence of Surface States," *Journal of the Electrochemical Society*, *123* (1976), 1828-1832.

[28] Laser, Daniel, and Allen J. Bard, "Semiconductor Electrodes: VIII. Digital Simulation of Open-Circuit Photopotentials," *Journal of the Electrochemical Society*, *123* (1976), 1833-1837.

[29] Laser, Daniel, and Allen J. Bard, "Semiconductor Electrodes: IX. Digital Simulation of the Relaxation of Photogenerated Free Carriers and Photocurrents," *Journal of the Electrochemical Society*, *123* (1976), 1837-1842.

[30] Laser, Daniel, "Modes of Charge Transfer at an Illuminated Semiconductor Electrode: a Digital Simulation," *Journal of the Electrochemical Society*, *126* (1979), 1011-1014.

[31] Leary, D. J., J. O. Barnes, and A. G. Jordan, "Calculation of Carrier Concentration in Polycrystalline Films as a Function of Surface Acceptor State Density: Application for ZnO Gas Sensors," *Journal of the Electrochemical Society*, *129* (1982), 1382-1386.

[32] Davis, James A., Robert O. James, and James O. Leckie, "Surface Ionization and Complexation at the Oxide-Water Interface: I. Computation of Electrical Double Layer Properties in Simple Electrolytes," *Journal of Colloid and Interface Science*, *63* (1978), 480-499.

[33] Davis, James A., and James O. Leckie, "Surface Ionization and Complexation at the Oxide-Water Interface: II. Surface Properties of Amorphous Iron Oxyhydroxide and Adsorption of Metal Ions," *Journal of Colloid and Interface Science*, *67* (1978), 91-107.

[34] Davis, James A., and James O. Leckie, "Surface Ionization and Complexation at the Oxide-Water Interface: 3. Adsorption of Ions," *Journal of Colloid and Interface Science*, *74* (1980), 32-43.

[35] Grahame, David C., "The Electrical Double Layer and the Theory of Electrocapillarity," *Chemical Reviews*, *41* (1947), 441-501.

[36] Dewald, J. F., "Semiconductor Electrodes," Chapter 17 in *Semiconductors*, N. B. Hannay, editor, Reinhold Publishing Corporation, New York, 1959.

[37] Sparnaay, Marcus Johannes, *The Electrical Double Layer*, Pergamon Press, New York, 1972.

[38] Parsons, Roger, "Equilibrium Properties of Electrified Interphases," Chapter 3 in *Modern Aspects of Electrochemistry*, Volume 1, John O'M Bockris, editor, Academic Press, New York, 1954, 103-179.

[39] Newman, John, *Electrochemical Systems*, Prentice-Hall, Inc., Englewood Cliffs, New Jersey, 1973.

[40] Gerischer, Heinz, "Semiconductor Electrochemistry," chapter 5 in *Physical Chemistry: An Advanced Treatise*, Volume IX, H. Eyring, editor, Academic Press, New York, 1970.

[41] Moll, John L., *Physics of Semiconductors*, McGraw-Hill Book Company, New York, 1964.

[42] Smith, R. A., *Semiconductors*, Cambridge University Press, London, 1959.

[43] Delahay, Paul, *Double Layer and Electrode Kinetics*, Interscience Publishers, New York, 1965.

[44] Orazem, Mark E. and John Newman, "Mathematical Modeling of Liquid-

Junction Photovoltaic Cells: II. Effect of System Parameters on Current-Potential Curves," submitted to *the Journal of the Electrochemical Society*, (LBL-16211).

[45] Orazem, Mark E. and John Newman, "Mathematical Modeling of Liquid-Junction Photovoltaic Cells: III. Optimization of Cell Configurations," submitted to *the Journal of the Electrochemical Society*, (LBL-16212).

TECHNICAL INFORMATION DEPARTMENT
LAWRENCE BERKELEY LABORATORY
UNIVERSITY OF CALIFORNIA
BERKELEY, CALIFORNIA 94720